



Condition Improvement for point relaxation in multigrid,
subsonic Euler-flow computations

B. Koren

Department of Numerical Mathematics

Report NM-R9413 June 1994

CWI is the National Research Institute for Mathematics and Computer Science. CWI is part of the Stichting Mathematisch Centrum (SMC), the Dutch foundation for promotion of mathematics and computer science and their applications.

SMC is sponsored by the Netherlands Organization for Scientific Research (NWO). CWI is a member of ERCIM, the European Research Consortium for Informatics and Mathematics.

Copyright © Stichting Mathematisch Centrum
P.O. Box 94079, 1090 GB Amsterdam (NL)
Kruislaan 413, 1098 SJ Amsterdam (NL)
Telephone +31 20 592 9333
Telefax +31 20 592 4199

Condition Improvement for Point Relaxation in Multigrid, Subsonic Euler-Flow Computations

Barry Koren
CWI

P.O. Box 94079, 1090 GB Amsterdam, The Netherlands

Abstract

Insight is given in the conditions of derivative matrices to be inverted in point-relaxation methods for 1-D and 2-D, upwind-discretized Euler equations. Speed regimes are found where ill-conditioning of these matrices occurs, 1-D flow equations appear to be less well conditioned than 2-D flow equations. Fixes to the ill conditions follow more or less directly, when thinking of adding regularizing matrices to the derivative matrices. A smoothing analysis is made of point Gauss-Seidel relaxation applied to the Euler equations conditioned by such an additive matrix. The conditioned solution method is successfully applied to a very low-subsonic, steady, 2-D stagnation flow.

AMS Subject Classification (1991): 65N12, 65N22, 65N55, 76G25, 76M25.

Keywords and Phrases: subsonic flows, Euler equations, multigrid methods, conditioning matrices, convergence.

Note: The research reported was performed in the framework of the BRITE-EURAM Aeronautics R&D Programme of the European Communities (Contract No. AER2-CT92-0040).

1 Introduction

The present paper is a sequel to [1] and [2]. In [1] a basic multigrid solution method for steady, upwind-discretized Euler equations was presented. In [2] some adaptations to this basic method were presented, particularly for hypersonic flow computations. In the present paper, some necessary adaptations are presented for low-subsonic flow computations.

In the incompressible limit, point-relaxation methods for solving discretized, steady Euler equations may suffer from ill-conditioning of the corresponding derivative matrices to be inverted. To see this, we start by considering the perfect-gas, steady, 1-D Euler equations

$$\frac{df(Q)}{dx} = 0, \quad (1a)$$

with Q the conservative state vector

$$Q = \begin{pmatrix} \rho \\ \rho u \\ \rho e \end{pmatrix}, \quad e = \frac{1}{\gamma - 1} \frac{p}{\rho} + \frac{1}{2} u^2, \quad (1b)$$

and $f(Q)$ the corresponding flux vector

$$f(Q) = \begin{pmatrix} \rho u \\ \rho u^2 + p \\ \rho u \left(e + \frac{p}{\rho} \right) \end{pmatrix}. \quad (1c)$$

Linearization of (1a) with respect to the conservative variables and, following [6], transformation from conservative variables Q to non-conservative (entropy) variables q ,

$$dq \equiv \begin{pmatrix} \frac{1}{\rho c} dp \\ du \\ dp - c^2 d\rho \end{pmatrix}, \quad (2)$$

yields the analytically tractable form

$$A \frac{dq}{dx} = 0, \quad (3a)$$

$$A = \frac{dq}{dQ} \frac{df}{dQ} \frac{dQ}{dq} = \begin{pmatrix} u & c & 0 \\ c & u & 0 \\ 0 & 0 & u \end{pmatrix}, \quad (3b)$$

$$\frac{df}{dQ} = \begin{pmatrix} 0 & 1 & 0 \\ \frac{\gamma-3}{2}u^2 & (3-\gamma)u & \gamma-1 \\ \frac{\gamma-2}{2}u^3 - \frac{1}{\gamma-1}uc^2 & \frac{(3-2\gamma)}{2}u^2 + \frac{1}{\gamma-1}c^2 & \gamma u \end{pmatrix}, \quad (3c)$$

$$\frac{dQ}{dq} = \begin{pmatrix} \frac{\rho}{c} & 0 & -\frac{1}{c^2} \\ \frac{\rho u}{c} & \rho & -\frac{u}{c^2} \\ \frac{1}{2} \frac{\rho u^2}{c} + \frac{1}{\gamma-1} \rho c & \rho u & -\frac{1}{2} \frac{u^2}{c^2} \end{pmatrix}. \quad (3d)$$

We proceed by considering a first-order upwind, cell-centered finite-volume discretization of (3a). Then, the discrete equation in cell Ω_i reads

$$A^+(q_i - q_{i-1}) + A^-(q_{i+1} - q_i) = 0, \quad (4)$$

with i running in positive x -direction, and with A^+ and A^- the matrices corresponding with the positive and negative eigenvalues of A :

$$A^+ = R_A \Lambda_A^+ R_A^{-1}, \quad A^- = R_A \Lambda_A^- R_A^{-1}. \quad (5)$$

With $\Lambda_A = \text{diag}(u - c, u, u + c)$ it holds

$$R_A = \begin{pmatrix} 1 & 0 & 1 \\ -1 & 0 & 1 \\ 0 & 1 & 0 \end{pmatrix}, \quad (6)$$

and, hence, for subsonic flow in positive x -direction, $0 < u < c$:

$$A^+ = \frac{1}{2} \begin{pmatrix} u+c & u+c & 0 \\ u+c & u+c & 0 \\ 0 & 0 & 2u \end{pmatrix}, \quad A^- = \frac{1}{2} \begin{pmatrix} u-c & c-u & 0 \\ c-u & u-c & 0 \\ 0 & 0 & 0 \end{pmatrix}. \quad (7)$$

Applying point Gauss-Seidel relaxation to find the solution q_i of (4), for successively a downstream and upstream relaxation sweep we have the iteration formulae

$$|A|(q_i^{n+1} - q_i^n) = -A^+(q_i^n - q_{i-1}^{n+1}) - A^-(q_{i+1}^n - q_i^n), \quad (8a)$$

$$|A|(q_i^{n+2} - q_i^{n+1}) = -A^+(q_i^{n+1} - q_{i-1}^{n+1}) - A^-(q_{i+1}^{n+2} - q_i^{n+1}), \quad (8b)$$

with n the relaxation sweep counter and $|A|$ the matrix to be inverted;

$$|A| \equiv A^+ - A^- = \begin{pmatrix} c & u & 0 \\ u & c & 0 \\ 0 & 0 & u \end{pmatrix}. \quad (9)$$

For $0 < u < c$, it holds

$$\Lambda_{|A|} = \text{diag}(c - u, u, u + c), \quad (10)$$

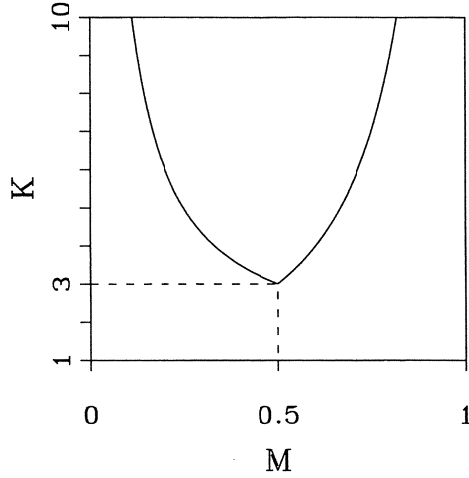


Figure 1: Condition of exact, 1-D absolute-eigenvalue matrix as a function of the Mach number.

and so $|A|$ has as condition over the entire subsonic flow regime

$$K_{|A|}(M) = \max\left(\frac{1+M}{M}, \frac{1+M}{1-M}\right), \quad M \equiv \frac{|u|}{c} \in (0, 1), \quad (11)$$

see also Figure 1. The best condition occurs at $M = \frac{1}{2}$; $K(M = \frac{1}{2}) = 3$, singularities occur at $M = 0$ and $M = 1$. Hence, in 1-D, in the neighborhood of the static and sonic flow conditions, when applying the iteration formulae (8a)-(8b), one may expect very large (too large) solution changes in case of very small right-hand sides only.

In 2-D numerical practice, ill-conditioning of derivative matrices to be inverted is not experienced in the neighborhood of $M = 1$, but only near $M = 0$. To get some evidence of this we also analyze the 2-D case. With $0 < u < c$, $0 < v < c$, a square finite volume, and j as additional running index in positive y -direction, one derives as iteration formulae for successively a downstream and upstream relaxation sweep:

$$(|A| + |B|)(q_{i,j}^{n+1} - q_{i,j}^n) = -A^+(q_{i,j}^n - q_{i-1,j}^{n+1}) - A^-(q_{i+1,j}^n - q_{i,j}^n) + \\ -B^+(q_{i,j}^n - q_{i,j-1}^{n+1}) - B^-(q_{i,j+1}^n - q_{i,j}^n), \quad (12a)$$

$$(|A| + |B|)(q_{i,j}^{n+2} - q_{i,j}^{n+1}) = -A^+(q_{i,j}^{n+1} - q_{i-1,j}^{n+1}) - A^-(q_{i+1,j}^{n+2} - q_{i,j}^{n+1}) + \\ -B^+(q_{i,j}^{n+1} - q_{i,j-1}^{n+1}) - B^-(q_{i,j+1}^{n+2} - q_{i,j}^{n+1}), \quad (12b)$$

with

$$A^+ = \frac{1}{2} \begin{pmatrix} u+c & u+c & 0 & 0 \\ u+c & u+c & 0 & 0 \\ 0 & 0 & 2u & 0 \\ 0 & 0 & 0 & 2u \end{pmatrix}, \quad A^- = \frac{1}{2} \begin{pmatrix} u-c & c-u & 0 & 0 \\ c-u & u-c & 0 & 0 \\ 0 & 0 & 0 & 0 \\ 0 & 0 & 0 & 0 \end{pmatrix}, \quad (13a)$$

$$B^+ = \frac{1}{2} \begin{pmatrix} v+c & 0 & v+c & 0 \\ 0 & 2v & 0 & 0 \\ v+c & 0 & v+c & 0 \\ 0 & 0 & 0 & 2v \end{pmatrix}, \quad B^- = \frac{1}{2} \begin{pmatrix} v-c & 0 & c-v & 0 \\ 0 & 0 & 0 & 0 \\ c-v & 0 & v-c & 0 \\ 0 & 0 & 0 & 0 \end{pmatrix}. \quad (13b)$$

So, in 2-D the matrix to be inverted is

$$|A| + |B| = A^+ - A^- + B^+ - B^- = \begin{pmatrix} 2c & u & v & 0 \\ u & v+c & 0 & 0 \\ v & 0 & u+c & 0 \\ 0 & 0 & 0 & u+v \end{pmatrix}. \quad (14)$$

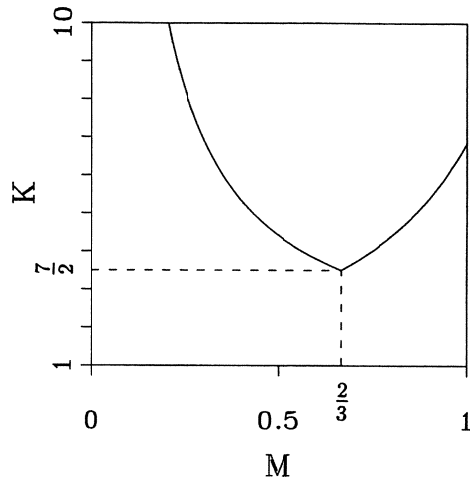


Figure 2: Condition of exact, 2-D absolute-eigenvalue matrix as a function of the Mach number.

For $\Lambda_{|A|+|B|}$ it holds when - without loss of generality - rotating in flow direction:

$$\Lambda_{|A|+|B|} = \text{diag} \left(\bar{u}, \frac{3}{2}c - \frac{1}{2}\sqrt{c^2 + 4\bar{u}^2}, \bar{u} + c, \frac{3}{2}c + \frac{1}{2}\sqrt{c^2 + 4\bar{u}^2} \right),$$

$$\bar{u} \equiv u \cos \phi + v \sin \phi, \quad \phi \equiv \arctan \frac{v}{u}, \quad (15)$$

and thus

$$K_{|A|+|B|}(M) = \max \left(\frac{3 + \sqrt{1 + 4M^2}}{2M}, \frac{3 + \sqrt{1 + 4M^2}}{3 - \sqrt{1 + 4M^2}} \right), \quad M \equiv \frac{|\bar{u}|}{c} \in (0, 1), \quad (16)$$

see also Figure 2. We see that in 2-D the singularity at $M = 1$ no longer exists, which explains the aforementioned numerical experience (i.e. the non-failure of the solution method presented in [1] for transonic flow computations). The best condition occurs at $M = \frac{2}{3}$, $K(M = \frac{2}{3}) = \frac{7}{2}$.

In the remainder of this paper, we discuss possible fixes to the 1-D and 2-D ill-conditionings of the absolute-eigenvalue matrices (Section 2), analyze the multigrid smoothing properties of a favorite fix (Section 3) and do some numerical experiments (Section 4). The difference with conditioning work as reviewed in [7] is that whereas in [7] conditions of the genuine Jacobian matrices are improved, here the conditions of absolute-eigenvalue Jacobians are improved.

2 Fixes to ill conditions of subsonic, absolute-eigenvalue matrices

2.1 Trimming 2-D singular matrix

For 2-D low-Mach-number flows, the equations (12a)-(12b) can be simply regularized by (locally) dropping the entropy-equation part, and by replacing that - in case of e.g. (12a) by either the homentropic iteration formula

$$s_{i,j}^{n+1} - s_{i,j}^n \equiv (p_{i,j}^{n+1} - p_{i,j}^n) - (c_{i,j}^n)^2 (\rho_{i,j}^{n+1} - \rho_{i,j}^n) = 0, \quad (17a)$$

or - alternatively - the incompressible formula

$$s_{i,j}^{n+1} - s_{i,j}^n = p_{i,j}^{n+1} - p_{i,j}^n. \quad (17b)$$

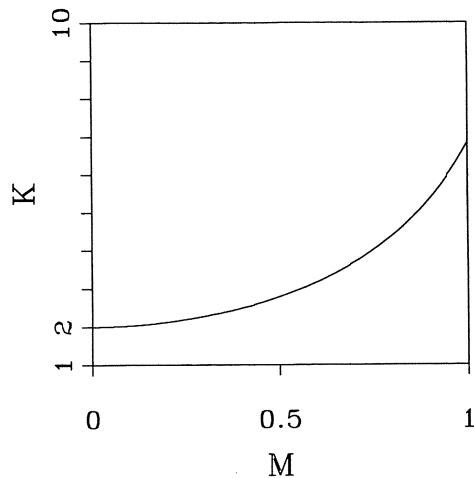


Figure 3: Condition of trimmed, 2-D, absolute-eigenvalue matrix as a function of the Mach number.

Dropping the entropy equation from system (12a)-(12b), the corresponding derivative matrix to be inverted reduces to

$$|A| + |B| = \begin{pmatrix} 2c & u & v \\ u & v + c & 0 \\ v & 0 & u + c \end{pmatrix}, \quad (18)$$

with, rotating again in flow direction

$$\Lambda_{|A|+|B|} = \text{diag} \left(\frac{3}{2}c - \frac{1}{2}\sqrt{c^2 + 4\bar{u}^2}, \bar{u} + c, \frac{3}{2}c + \frac{1}{2}\sqrt{c^2 + 4\bar{u}^2} \right), \quad (19)$$

and thus

$$K_{|A|+|B|}(M) = \frac{3 + \sqrt{1 + 4M^2}}{3 - \sqrt{1 + 4M^2}}, \quad M \in (0, 1), \quad (20)$$

see also Figure 3. A difficulty of splitting off the singular part from the iteration formulae in case of general subsonic flows is that it requires the introduction of a monitor for switching on and off homentropy or incompressibility, i.e. (17a) or (17b). Rigorous formulae for setting thresholds for the monitors are hard to derive. Therefore we refrain from applying these reduced derivative matrices.

2.2 Adding 1-D and 2-D regularizing matrices

Considering the 1-D absolute-eigenvalue matrix (9), it can be regularized by adding a matrix R to it, leading to the approximate derivative matrix:

$$|A|_R \equiv |A| + R. \quad (21)$$

Taking

$$R = \alpha \begin{pmatrix} 0 & -u & 0 \\ 0 & 0 & 0 \\ 0 & 0 & c - u \end{pmatrix} \quad \text{or} \quad R = \alpha \begin{pmatrix} 0 & 0 & 0 \\ -u & 0 & 0 \\ 0 & 0 & c - u \end{pmatrix}, \quad (22)$$

for any constant $\alpha \in (0, 1]$ the singularities at $M = 0$ and $M = 1$ are removed. For both R 's from (22) we find

$$\Lambda_{|A|_R} = \text{diag}(c - \sqrt{1 - \alpha}u, \alpha c + (1 - \alpha)u, c + \sqrt{1 - \alpha}u), \quad (23)$$

and hence

$$K_{|A|_R}(M) = \max \left(\frac{1 + \sqrt{1 - \alpha}M}{\alpha + (1 - \alpha)M}, \frac{1 + \sqrt{1 - \alpha}M}{1 - \sqrt{1 - \alpha}M} \right), \quad M \in (0, 1), \quad \alpha \in (0, 1], \quad (24)$$

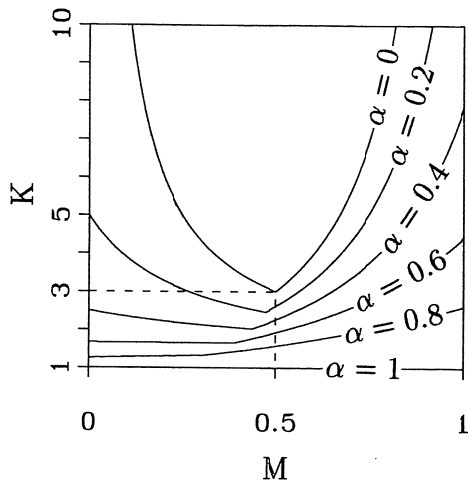


Figure 4: Condition of through addition regularized, 1-D absolute-eigenvalue matrix, as a function of the Mach number.

see also Figure 4. For $\alpha = 1$, $|A|_R$ is perfectly well-conditioned over the entire subsonic Mach-number range, whereas the corresponding approximate derivative matrix $|A|_R$ will generally be rather close to the exact derivative matrix $|A|$. A convergence requirement to be satisfied is that the eigenvalues of $|A|_R$ are positive. This requirement is met by both R 's from (22), for any $\alpha \in (0, 1]$.

In 2-D, where no sonic singularity exists, to regularize (14) we may take

$$R = \alpha \begin{pmatrix} 0 & 0 & 0 & 0 \\ 0 & 0 & 0 & 0 \\ 0 & 0 & 0 & 0 \\ 0 & 0 & 0 & c - u - v \end{pmatrix}, \quad \alpha \in (0, 1]. \quad (25)$$

So, in 2-D we have the advantage of remaining closer to the exact derivative matrix than in 1-D. For the corresponding eigenvalue-matrix $\Lambda_{(|A|+|B|)_R}$ it holds

$$\Lambda_{(|A|+|B|)_R} = \text{diag} \left(\alpha c + (1 - \alpha)\bar{u}, \frac{3}{2}c - \frac{1}{2}\sqrt{c^2 + 4\bar{u}^2}, \bar{u} + c, \frac{3}{2}c + \frac{1}{2}\sqrt{c^2 + 4\bar{u}^2} \right), \quad (26)$$

and hence

$$K_{(|A|+|B|)_R}(M) = \max \left(\frac{3 + \sqrt{1 + 4M^2}}{2(\alpha + (1 - \alpha)M)}, \frac{3 + \sqrt{1 + 4M^2}}{3 - \sqrt{1 + 4M^2}} \right), \quad M \in (0, 1), \quad \alpha \in (0, 1], \quad (27)$$

see also Figure 5. As opposed to the preceding 1-D conditioning, which is perfect for $\alpha = 1$, perfect 2-D conditioning through (25) is not possible. In the next section, for 2-D flows, we will investigate the multigrid smoothing (high-frequency damping) properties of point Gauss-Seidel relaxation when applying additive conditioning. For reasons of transparency, smoothing properties are investigated for the 1-D equation.

3 Smoothing analysis of additive conditioning

Consider the downstream iteration formula

$$(R + |A|)(q_i^{n+1} - q_i^n) = -A^+(q_i^n - q_{i-1}^{n+1}) - A^-(q_{i+1}^n - q_i^n), \quad (28a)$$

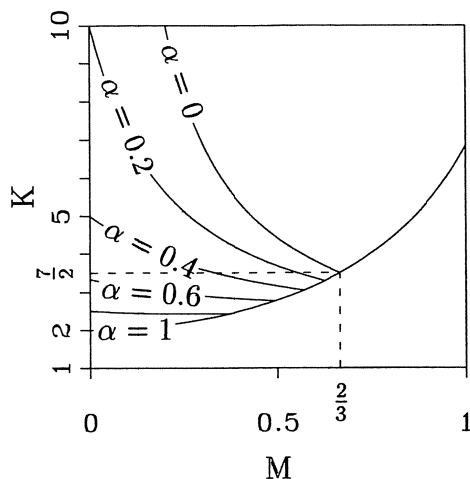


Figure 5: Condition of through addition regularized, 2-D absolute-eigenvalue matrix as a function of the Mach number.

and the upstream formula

$$(R + |A|)(q_i^{n+2} - q_i^{n+1}) = -A^+(q_i^{n+1} - q_{i-1}^{n+1}) - A^-(q_{i+1}^{n+2} - q_i^{n+1}), \quad (28b)$$

where R is the 1-D equivalent of the 2-D additive matrix (25):

$$R = \alpha \begin{pmatrix} 0 & 0 & 0 \\ 0 & 0 & 0 \\ 0 & 0 & c - u \end{pmatrix}. \quad (29)$$

To investigate the smoothing properties, the local solution error

$$\delta_i^n = q_i^* - q_i^n, \quad (30a)$$

and its Fourier form

$$\delta_i^n = D^n e^{i\theta}, \quad |\theta| \in \left[\frac{\pi}{2}, \pi\right] \quad (30b)$$

are introduced. In here, q_i^* is the exact local solution, D^n the amplitude vector (D_1^n, D_2^n, D_3^n) and $e^{i\theta}$ the (scalar) mode. Keeping the coefficient matrices in (28a) and (28b) frozen, with (30a) and (30b), from (28a) and (28b) it follows for the corresponding amplification matrices $\mathcal{M}_{\text{downstream}}$ and $\mathcal{M}_{\text{upstream}}$:

$$\mathcal{M}_{\text{downstream}} = (R + (1 - e^{-i\theta})A^+ - A^-)^{-1} (R - e^{i\theta}A^-), \quad (31a)$$

$$\mathcal{M}_{\text{upstream}} = (R + A^+ - (1 - e^{i\theta})A^-)^{-1} (R + e^{-i\theta}A^+). \quad (31b)$$

In both $\mathcal{M}_{\text{downstream}}$ and $\mathcal{M}_{\text{upstream}}$ the influence of α is confined to a single eigenvalue per matrix only:

$$\lambda_{\mathcal{M}_{\text{downstream}}}(\alpha) = \frac{\alpha(1 - M)}{\alpha(1 - M) + (1 - e^{-i\theta})M}, \quad (32a)$$

$$\lambda_{\mathcal{M}_{\text{upstream}}}(\alpha) = \frac{\alpha(1 - M) + e^{-i\theta}M}{\alpha(1 - M) + M}. \quad (32b)$$

It can be seen that for $\alpha = 1$, it still holds

$$|\lambda_{\mathcal{M}_{\text{downstream}}}(\alpha = 1)| \leq 1 \quad \text{and} \quad |\lambda_{\mathcal{M}_{\text{upstream}}}(\alpha = 1)| \leq 1, \quad \forall |\theta| \in \left[\frac{\pi}{2}, \pi\right], \quad \forall M \in (0, 1). \quad (33)$$

We assume that $\alpha = 1$ is an acceptable choice in 2-D as well. In the next section the conservative implementation of the 2-D additive conditioning is discussed and some numerical results, obtained for a 2-D stagnation flow, are given.

4 Application of additive conditioning

4.1 2-D conservative implementation

Discretizing the steady, 2-D, conservative Euler equations by a first-order upwind, cell-centered finite-volume method, and denoting the numerical flux functions which approximate the cell-face fluxes in x - and y -direction ($f(q_{i+\frac{1}{2},j})$ and $g(q_{i,j+\frac{1}{2}})$) by $F(q_{i,j}, q_{i+1,j})$ and $G(q_{i,j}, q_{i,j+1})$, respectively, the conservative upstream and downstream relaxation sweeps read:

$$\begin{aligned} & \left[\frac{dQ}{dq}(q_{i,j}^n) R(q_{i,j}^n) \bar{h}_{i,j} + \frac{\partial F(q_{i,j}^n, q_{i+1,j}^n)}{\partial q_{i,j}^n} h_{i+\frac{1}{2},j} - \frac{\partial F(q_{i-1,j}^n, q_{i,j}^n)}{\partial q_{i,j}^n} h_{i-\frac{1}{2},j} + \right. \\ & \quad \left. + \frac{\partial G(q_{i,j}^n, q_{i,j+1}^n)}{\partial q_{i,j}^n} h_{i,j+\frac{1}{2}} - \frac{\partial G(q_{i,j-1}^n, q_{i,j}^n)}{\partial q_{i,j}^n} h_{i,j-\frac{1}{2}} \right] (q_{i,j}^{n+1} - q_{i,j}^n) = \\ & \quad F(q_{i-1,j}^{n+1}, q_{i,j}^n) h_{i-\frac{1}{2},j} - F(q_{i,j}^n, q_{i+1,j}^n) h_{i+\frac{1}{2},j} \\ & \quad + G(q_{i,j-1}^{n+1}, q_{i,j}^n) h_{i,j-\frac{1}{2}} - G(q_{i,j}^n, q_{i,j+1}^n) h_{i,j+\frac{1}{2}}, \end{aligned} \quad (34a)$$

$$\begin{aligned} & \left[\frac{dQ}{dq}(q_{i,j}^{n+1}) R(q_{i,j}^{n+1}) \bar{h}_{i,j} + \frac{\partial F(q_{i,j}^{n+1}, q_{i+1,j}^{n+1})}{\partial q_{i,j}^{n+1}} h_{i+\frac{1}{2},j} - \frac{\partial F(q_{i-1,j}^{n+1}, q_{i,j}^{n+1})}{\partial q_{i,j}^{n+1}} h_{i-\frac{1}{2},j} + \right. \\ & \quad \left. + \frac{\partial G(q_{i,j}^{n+1}, q_{i,j+1}^{n+1})}{\partial q_{i,j}^{n+1}} h_{i,j+\frac{1}{2}} - \frac{\partial G(q_{i,j-1}^{n+1}, q_{i,j}^{n+1})}{\partial q_{i,j}^{n+1}} h_{i,j-\frac{1}{2}} \right] (q_{i,j}^{n+2} - q_{i,j}^{n+1}) = \\ & \quad F(q_{i-1,j}^{n+1}, q_{i,j}^{n+1}) h_{i-\frac{1}{2},j} - F(q_{i,j}^{n+1}, q_{i+1,j}^{n+1}) h_{i+\frac{1}{2},j} \\ & \quad + G(q_{i,j-1}^{n+1}, q_{i,j}^{n+1}) h_{i,j-\frac{1}{2}} - G(q_{i,j}^{n+1}, q_{i,j+1}^{n+1}) h_{i,j+\frac{1}{2}}, \end{aligned} \quad (34b)$$

where $\bar{h}_{i,j}$ is a cell-averaged mesh width, e.g. $\bar{h}_{i,j} = \frac{1}{4} (h_{i-\frac{1}{2},j} + h_{i+\frac{1}{2},j} + h_{i,j-\frac{1}{2}} + h_{i,j+\frac{1}{2}})$, and where

$$\frac{dQ}{dq} = \begin{pmatrix} \frac{\rho}{c} & 0 & 0 & -\frac{1}{c^2} \\ \frac{\rho u}{c} & \rho & 0 & -\frac{u}{c^2} \\ \frac{\rho v}{c} & 0 & \rho & -\frac{v}{c^2} \\ \frac{1}{2} \frac{\rho(u^2+v^2)}{c} + \frac{1}{\gamma-1} \rho c & \rho u & \rho v & -\frac{1}{2} \frac{u^2+v^2}{c^2} \end{pmatrix}, \quad (35)$$

yielding

$$\frac{dQ}{dq} R = \begin{pmatrix} 0 & 0 & 0 & -\frac{c-u-v}{c^2} \\ 0 & 0 & 0 & -\frac{u(c-u-v)}{c^2} \\ 0 & 0 & 0 & -\frac{v(c-u-v)}{c^2} \\ 0 & 0 & 0 & -\frac{1}{2} \frac{(u^2+v^2)(c-u-v)}{c^2} \end{pmatrix}. \quad (36)$$

4.2 Numerical results

A suitable test case is steady, 2-D stagnation flow normal to a flat plate (Figure 6). A favorable property of this test case is the direct availability of good approximate boundary conditions (because of the availability of an exact, incompressible potential flow solution, see e.g. Chapter X from [5]). For computational efficiency, we only compute the half problem ($x \geq 0$). (We remark that exact solutions of subsonic flows along a kinked wall have a singularity at the kink for all kink angles δ except $\delta = 0$ and $\delta = \frac{\pi}{2}$, which latter case is identical to the present normal stagnation flow.) Introducing as known quantities in the point $(x, y) = (1, 1)$: a reference speed w_{ref} , a reference density ρ_{ref} , and a reference Mach number M_{ref} , the boundary conditions imposed are:

- at the inflow boundary, assuming homenthalpy:

$$u(x, y = 1) = w_{\text{ref}} x, \quad (37)$$

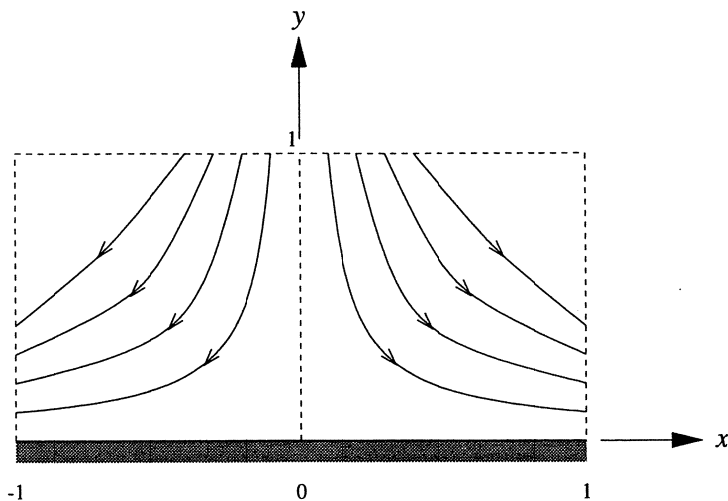


Figure 6: Stagnation flow against a flat plate.

$$v(x, y = 1) = -w_{\text{ref}}, \quad (38)$$

$$c(x, y = 1) = \sqrt{\frac{w_{\text{ref}}^2}{M_{\text{ref}}^2} + \frac{\gamma - 1}{2} (w_{\text{ref}}^2 - u^2(x, y = 1) - v^2(x, y = 1))}, \quad (39)$$

- at the outflow boundary, assuming homentropy and homenthalpy:

$$p(x = 1, y) = \left(1 + \frac{\gamma - 1}{2} \frac{w^2(x = 1, y)}{c^2(x = 1, y)}\right)^{-\frac{\gamma}{\gamma - 1}} p_t, \quad (40a)$$

where

$$w^2(x = 1, y) = w_{\text{ref}}^2(1 + y^2), \quad (40b)$$

$$c^2(x = 1, y) = \frac{w_{\text{ref}}^2}{M_{\text{ref}}^2} + \frac{\gamma - 1}{2} (w_{\text{ref}}^2 - w^2(x = 1, y)), \quad (40c)$$

$$p_t = \left(1 + \frac{\gamma - 1}{2} M_{\text{ref}}^2\right)^{\frac{\gamma}{\gamma - 1}} p_{\text{ref}}, \quad p_{\text{ref}} = \frac{1}{\gamma} \frac{w_{\text{ref}}^2}{M_{\text{ref}}^2} \rho_{\text{ref}}, \quad (40d)$$

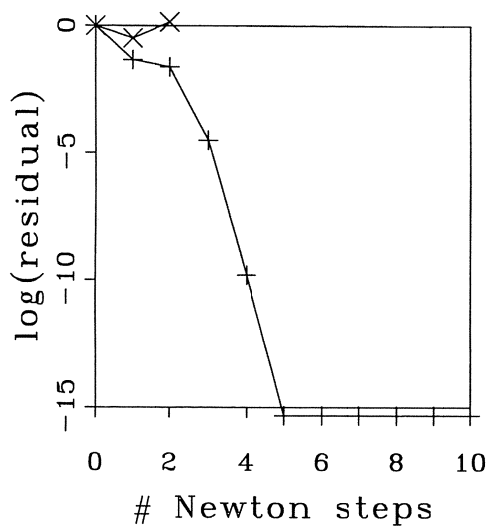
- at the vertical-wall boundary:

$$u(x = 0, y) = 0, \quad (41)$$

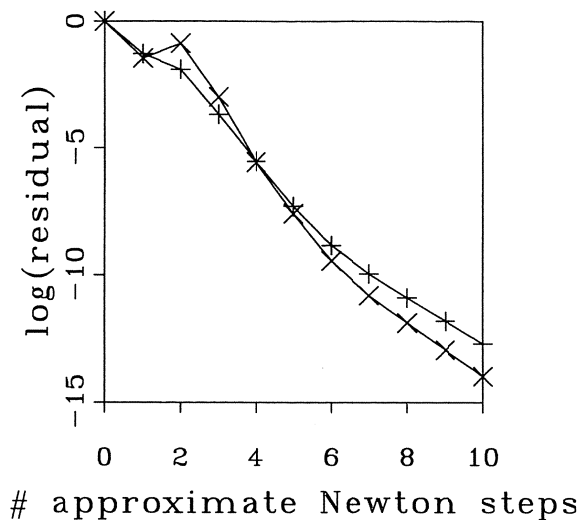
- at the lower-wall boundary:

$$v(x, y = 0) = 0. \quad (42)$$

In Figure 7, for two low-subsonic (though not yet very low-subsonic) values of M_{ref} , we give the convergence behaviors of the point relaxation in some arbitrary cell, at some arbitrary instant in the iteration process. (The residual considered is that of the energy equation.) From the results it appears that the additive conditioning does a good job. Though quadratic convergence is lost, the divergence as occurring at $M_{\text{ref}} = 0.075$ (Figure 7a) has disappeared by applying the conditioning (Figure 7b). In Figure 8, convergence results are presented, as obtained through the conditioned relaxation method accelerated by nonlinear multigrid. (The residual considered is the L_{∞} -norm of the energy equation's residual field.) The Mach-number sequence considered is: $M_{\text{ref}} = 0.5, 0.05, 0.005$. Note that the method does not break down, but still converges in the very low-subsonic case $M_{\text{ref}} = 0.005$. The decrease of convergence rates at decreasing Mach numbers that can be observed, is related to the decreasing entropy-error convection across domain boundaries. Fixing this requires the condition improvement of the Jacobians. As mentioned, a review of such techniques is given in [7]. (An early research paper in the context of single-grid, explicit time-stepping schemes is [4], and a multigrid, locally implicit extension of this is [3].)

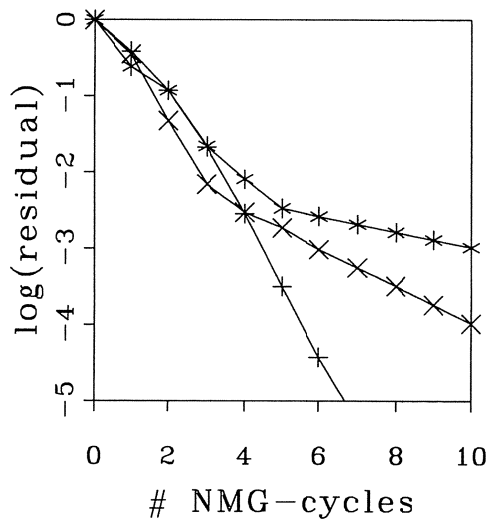


a. Without conditioning.

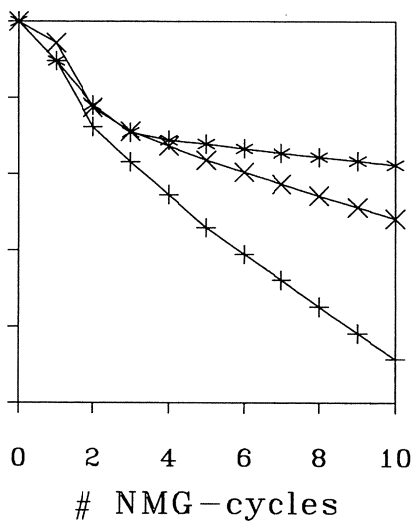


b. With conditioning.

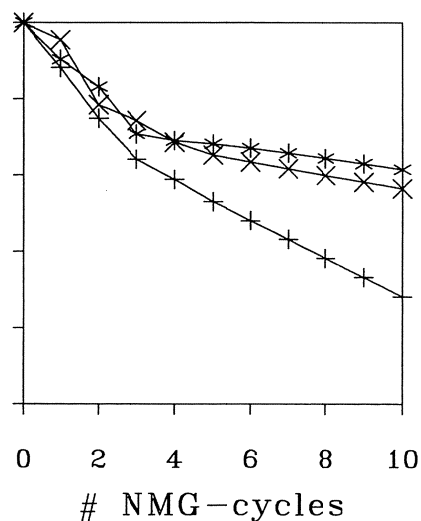
Figure 7: Convergence behaviors point relaxation, +: $M_{\text{ref}} = 0.1$, \times : $M_{\text{ref}} = 0.075$.



a. $M_{\text{ref}} = 0.5$.



b. $M_{\text{ref}} = 0.05$.



c. $M_{\text{ref}} = 0.005$.

Figure 8: Convergence behaviors nonlinear multigrid iteration, +: $h = \frac{1}{8}$, \times : $h = \frac{1}{16}$, *: $h = \frac{1}{32}$.

5 Conclusions

Two methods have been proposed for removing singularities in local, absolute-eigenvalue matrices of upwind-discretized Euler equations:

- elimination of the entropy-equation part from the exact, 2-D derivative matrix;
- addition of a singular matrix (which is very close to the zero matrix) to the singular, exact derivative matrix.

The first fix does not work in 1-D. Another drawback is that its successful application requires tuning. The second fix is free of tuning parameters and may remove the ill-conditioning without deteriorating too much the quadratic convergence rate of exact Newton iteration. The latter fix has been successfully applied to a steady, 2-D, low-subsonic stagnation flow.

References

- [1] P.W. HEMKER AND S.P. SPEKREIJSE, Multiple grid and Osher's scheme for the efficient solution of the steady Euler equations, *Appl. Numer. Math.*, **2**, 475-493, 1986.
- [2] B. KOREN AND P.W. HEMKER, Damped, direction-dependent multigrid for hypersonic flow computations, *Appl. Numer. Math.*, **7**, 309-328, 1991.
- [3] B. KOREN, Preconditioning and multigrid for Euler flows with low-subsonic regions, CWI Report 94xx, 1994.
- [4] B. VAN LEER, W.-T. LEE AND P.L. ROE, Characteristic time-stepping or local preconditioning of the Euler equations, *AIAA-91-1552*, 1991.
- [5] L. PRANDTL AND O.G. TIETJENS, *Fundamentals of Hydro- and Aeromechanics*, Dover, New York, 1957.
- [6] E. TURKEL, Preconditioned methods for solving the incompressible and low speed compressible equations, *J. Comput. Phys.*, **72**, 277-298, 1987.
- [7] E. TURKEL, Review of preconditioning methods for fluid dynamics, *Appl. Numer. Math.*, **12**, 257-284, 1993.

Contents

1	Introduction	1
2	Fixes to ill conditions of subsonic, absolute-eigenvalue matrices	4
2.1	Trimming 2-D singular matrix	4
2.2	Adding 1-D and 2-D regularizing matrices	5
3	Smoothing analysis of additive conditioning	6
4	Application of additive conditioning	8
4.1	2-D conservative implementation	8
4.2	Numerical results	8
5	Conclusions	11